# Large effect life-history genomic regions are associated with functional morphological traits in Atlantic salmon

Tutku Aykanat[1], Paul V. Debes[2,6], Shadi Jansouz[1], Lison Gueguen[3], Andrew H. House[1], Annukka Ruokolainen[1], Jaakko Erkinaro[4], Victoria L. Pritchard[5], Craig R. Primmer[1,6], Geir H. Bolstad[7]

1. Organismal and Evolutionary Biology Research Program, Faculty of Biological and Environmental Sciences, PO Box 56, FI-00014 University of Helsinki, Finland. tutku.aykanat@helsinki.fi.
2. Department of Aquaculture and Fish Biology, Hólar University, 550 Sauðárkrókur, Iceland.
3. Oniris Graduate School of Veterinary Medicine, Nantes, France.
4. Natural Resources Institute Finland (Luke), Oulu, Finland
5. Institute for Biodiversity & Freshwater Conservation, UHI Inverness, Inverness, United Kingdom., United Kingdom.
6. Institute of Biotechnology, Helsinki Institute of Life Science (HiLIFE), University of Helsinki, Helsinki, Finland.
7. Norwegian Institute for Nature Research (NINA), NO-7485 Trondheim, Norway.

**Short running title:** Functional morphology linked to major life history loci

**Keywords:** Atlantic salmon, morphology, morphometrics, adaptive genetic variation, age at maturity, pleiotropy, *six6*, *vgll3*

## Abstract

Understanding pleiotropic architectures of phenotypes is instrumental for identifying the functional basis of adaptive genetic variation in the wild. Life-history variation may have a morphological basis that mediates resource acquisition allocation pathways, but identifying the underlying genetic basis of such traits is challenging. Using Atlantic salmon juveniles reared in common garden conditions, we test if two life-history associated loci in Atlantic salmon, s*ix6* and *vgll3,* are also associated with functional morphological traits. These loci had previously shown to exhibit strong signals of adaptation and are highly correlated with sea age at maturity. We show that genetic variation at the *vgll3* locus is linked to variation in morphological traits that underlie swimming performance, along a trade-off axis between efficient cruising and maneuvering, while the genetic variation at the *six6* locus was linked to variation in body-head proportions suggesting the potential functional importance of these traits for resource acquisition efficiency. However, the direction of changes in morphological traits associated with late- vs. early- maturing alleles was not always consistent with the expected direction of an effect to maturation timing. Our results reveal a complex morphological landscape associated with the genetic variation in these loci, possibly as a result of pleiotropy or linkage across these genomic regions.



**Keywords:** Atlantic salmon, morphology, morphometrics, adaptive genetic variation, age at maturity, pleiotropy, *six6*, *vgll3*

## Introduction

Elucidating the genotype-phenotype relationship is instrumental in identifying the functional basis of adaptation and the potential targets of selection (Barrett and Hoekstra, 2011; Kawecki and Ebert, 2004; Nielsen *et al*, 2009; Wagner and Altenberg, 1996). Methodological and statistical advances in genetics now allow the identification of genomic regions responding to local selection, but the phenotypic link between genotype and fitness is often missing. Furthermore, many genomic regions can affect a multitude of phenotypic traits (via pleiotropy or linkage disequilibrium), which makes identifying the phenotypic traits under selection even more challenging (Paaby and Rockman, 2013; Solovieff *et al*, 2013). Even large, genome-wide association studies might be underpowered to detect pleiotropy (Wagner and Zhang, 2011), a methodological bias by which the adaptive significance of pleiotropy can be overlooked especially in natural, non-model populations even if it may have substantial effects to limit or promote adaptation (Orr, 2000; Otto, 2004). In natural systems, pleiotropy has been mostly studied at the phenotypic level to understand the evolutionary trade-offs by quantifying the physiological antagonisms between senescence and reproduction age. Yet, some studies identify pleiotropic effects of genes associated with adaptive genetic variation. For example, adaptive divergence between lake vs. marine morphs of threespine stickleback (*Gasterosteus aculeatus*) was explained by both pleiotropy in the *Eda* gene, and via strong linkage with the surrounding loci (Archambeault *et al*, 2020), illustrating the significance of such genetic architectures for adaptation.

Genomic regions with large adaptive importance are more likely to be detected in genome scans and are likely to have broad cellular and phenotypic effects (Shapiro *et al*, 2003, Jones *et al*, 2012, , Barson *et al*, 2015). Major effect loci may also have broad cellular and phenotypic effects, with key regulatory roles across development, and could thereby drive strong genetic interdependences among traits (Chan *et al*, 2010; Colosimo *et al*, 2005; Jimenez-Gomez *et al*, 2010; Weith *et al*, 2023) but see (Boyle *et al*, 2017; Jakobson and Jarosz, 2020). Therefore, loci exhibiting strong signals of adaptation may provide feasible empirical approaches to understand the significance of complex evolutionary processes, such as how pleiotropy and genetic interactions may hinder or promote adaptation in relation to the direction of natural selection between co-varying traits. Yet, such examples remain rare in non-model, wild organisms (Archambeault *et al*, 2020; Endler, 2000; Mackay *et al*, 2009; Olson-Manning *et al*, 2012).

Functional variation in morphological traits is integral in shaping resource use, and is correspondingly associated with life-history variation and ecotypic divergence in a large array of fish species, including salmonid fishes (Ferry-Graham *et al*, 2002; Fitzgerald *et al*, 2017; Keeley *et al*, 2005; Lundsgaard-Hansen *et al*, 2013; Mindel *et al*, 2016; Proulx and Magnan, 2004; Svanbäck and Eklöv, 2003; Taylor and McPhail, 1985; Varian and

67 Nichols, 2010; Webb, 1988). For example, a fusiform body and shorter fins appear adaptive to a long-distance
68 migratory strategy, likely because this body shape reduces the drag (hence the energy consumed) during
69 migration (Morinville and Rasmussen, 2007). Likewise, a robust body shape with a larger head, caudal
70 peduncle, and paired fins has been associated with piscivory in rainbow trout (*Oncorhynchus mykiss*, Keeley *et*
71 *al*, 2005). Recent population genomics studies in Atlantic salmon have consistently identified two unlinked
72 genomic regions, surrounding the genes *six6* in chromosome 9 and *vgll3* in chromosome 25 as strong targets
73 for local selection within all European Atlantic salmon lineages (Barson *et al*, 2015; Miettinen *et al*, 2023;
74 Pritchard *et al*, 2018; Zueva *et al*, 2020). These two loci have also been linked to a suite of life-history traits that
75 strongly influence fitness. In particular, the *vgll3* and *six6* loci are strongly associated with sea age at first
76 maturity (age at maturity from here on) in seagoing salmon at the individual- and population- levels
77 respectively (Barson *et al*, 2015, see also, Ayllon *et al*, 2015; Sinclair-Waters *et al*, 2020), and the *vgll3* locus
78 affects other alternative life-history strategies, such as precocious male maturation (Debes *et al*, 2021), and
79 iteroparity (Aykanat *et al*, 2019). For example, individuals with late maturation genotype in the *vgll3* gene
80 ($vgll3^{LL}$) tended to stay at sea, on average, more than one year more than individuals with early maturation
81 ($vgll3^{EE}$) genotype (Barson *et al*, 2015, Mobley *et al*, 2021). This pattern was also pertinent during the
82 freshwater phase within which juvenile males with $vgll3^{LL}$ genotype matured at a much higher probability (~
83 60%) than juvenile males with $vgll3^{LL}$ genotype (Debes *et al*, 2021).

84 Similarly, these loci explain variation across a number of metabolic and behavior traits. For example, $vgll3^{E}$
85 allele has been shown to be associated with reduced aggression, increased maximum metabolic rate and
86 aerobic scope at the juvenile stage (Bangura *et al*, 2022; Prokkola *et al*, 2022), while *six6* locus predicts diet
87 acquisition patterns at sea in maturing adults with $six6^{E}$ allele linked to increased stomach weight despite
88 decreased foraging efforts (Aykanat *et al*, 2020). Likewise, *six6* locus exhibits epistasis with *vgll*3 to affect
89 aerobic scope variation (Prokkola *et al*, 2022). The strong genetic interdependence of these phenotypic traits
90 across two loci points to the potential for a shared developmental origin (of phenotypes to the respective loci),
91 which is supported by the role of *vgll3* and *six6* in the hormonal and cell-fate commitment gene-expression
92 pathways (Ahi *et al*, 2022; Kurko *et al*, 2020; Verta *et al*, 2020; Verta *et al*, 2024) and broad expression of *six6*
93 during early development (Moustakas-Verho *et al*, 2020). Finally, a recent study showed both loci are linked to
94 early life survival in juvenile Atlantic salmon, albeit via parental genetic effects, further supporting broad
95 functional roles across life stages (Aykanat *et al*, 2024). This collective evidence indicates that these loci are
96 broad-scale modulators of salmon phenotype. While many of these genetic effects have been demonstrated
97 for traits at the juvenile stage, including early male maturation, metabolism, and behavior, any concordance

98 with morphological variation, if any, is not known, but may be important to identify the architecture of
99 personality traits, underlying genetic basis, and evolutionary constrains (Bangura *et al*, 2022, Kern et al, 2016).

100 To characterize the morphological variation associated with these locally adaptive genomic regions, we collected
101 morphometric data form more than 700 juvenile immature Atlantic salmon at time when male parr maturation
102 may take place (Debes *et al*, 2021). The fish was reared in common garden conditions and the association
103 between morphology, and *six6* and *vgll3* genotype was estimated with a mixed-effect model that also controls for
104 confounding length and condition factor effects. We identified a suite of morphological characters correlated to
105 the genetic variation in both loci. Our study extends the broad pleiotropic effect of *vgll3* and *six6* loci to functional
106 morphological traits, including phenotypes that are likely important targets of natural selection.

107

## 108 Materials and Methods

109 *Fish breeding and, rearing and common garden conditions*

110 Details of the breeding and rearing of individuals from the same cohort were provided in Debes *et al* (2021),
111 using a similar experimental procedure and facilities, except that the fish in the present study were reared in
112 approximately 2°C cooler water temperature (see, Debes *et al* (2019) for the details of the rearing
113 temperature). Briefly, the parents of the individuals used were from Baltic lineage Atlantic salmon from a
114 broodstock maintained by the Natural Resources Institute Finland (Laukaa, Finland) that were initially
115 originated from the Neva River in Russia (Gulf of Finland in the Eastern Baltic Sea) and has been used for
116 juvenile salmon supplementation in the Kymi river in South-Eastern Finland (Asheim *et al*, 2023). Parents were
117 crossed using a biallelic cross design where 44 parents were crossed in a 11 two by two factorials design, in
118 which, each factorial unit composed of a pair of males and females which are homozygote in early (E) and late
119 (L) maturing alleles in the *vgll3* locus (i.e. *vgll3*$^{EE}$ and *vgll3*$^{LL}$ genotypes, Supplementary Table 1), with one type
120 of genotype within each of the full-sib families with EE, EL, LE, and LL genotypes in the *vgll3* locus
121 (Supplementary Table 1). *Six6* genotype distribution was not considered during the breeding design, but was
122 nevertheless segregating in a number of families (Supplementary Table 1). Crosses were performed in
123 November 2017, and offspring were reared in the University of Helsinki fish facilities, first in replicated family-
124 specific compartments in vertical incubators until the swim-up stage. Subsequently offspring of all families
125 were mixed in eight tanks with roughly balanced proportions of families per tank (Supplementary Table 2). In
126 August 2018, fish were pit-tagged when and fin-clipped for later genotyping. Genotyping and genotypic sex of
127 the parent and offspring were performed by genotyping-by-sequencing using 177 nucleotide polymorphisms

128 (SNPs) which included *vgll3* and *six6* SNPs, which were also used for parentage assignment (see, Debes *et al,*
129 2021, for details). The rearing temperature of the fish in this study followed a seasonal cycle (range: 4.1–
130 16.0°C) and the natural light regime of the latitude (61.054° N) as described in Debes *et al* (2019). In August
131 2018, the fish were individually PIT-tagged and a fin clip sample was taken to identify the families via genetic
132 pedigree reconstruction. Fish were fed ad libitum except for a short period of restricted feeding for half of the
133 tanks, which included ad libitum feeding for two days and then no feeding for five days, each week for a five-
134 week period (Debes *et al*, 2021).

135 *Landmarking and trait measurements*

136 Morphological data were collected as part of a larger effort in December 2018. Fish of both sexes were
137 euthanized using an overdose of tricaine methanesulphonate bath, and stored briefly on ice until imaging was
138 performed the same day. Each fish was sliced ventrally to collect data on gonad development for another
139 study. The fish was placed on graphical paper, and the body image was taken using a digital camera (Canon
140 PowerShot S110) mounted on a tripod (Hama Star 61), with aperture-priority exposure at F:8, with autofocus
141 option (Supplementary Figure 1). Cross sections were obtained by slicing the fish at the posterior end of the
142 dorsal fin (hereafter termed as large cross section) and adipose fins (hereafter termed as small cross section),
143 respectively. These were placed on a transparent sheet and digitized using a scanner (Epson XP-305) with a
144 modified lid to accommodate the depth of the cross sections (Supplementary Figure 1).

145 Landmarks were placed on the whole body and the two cross sections in a randomized order using imglab
146 software (King, 2009), by two of the co-authors (LG for landmarked body planes, and SC for landmarked cross
147 sections) who were blind to any information related to the genotypes or sex of the fish (Supplementary Figure
148 2). Landmarks were not placed around the gut region due to the previous ventral slicing. Some landmarks were
149 solely used in the Procrustes analysis to quantify shape, while others were used to quantify specific trait values
150 by calculating the distance between landmarks (Supplementary Figure 2, Table 1). Traits that were measured
151 twice along the transverse plane (both the left and right sides, Table 1) were averaged prior to analysis. All
152 measurements were reported in centimeters (cm).

153 *Data filtering*

154 At the time of sampling, fish exhibited a bimodal length distribution which is often observed within juvenile
155 salmon from the same cohort (Hoar, 1988). At the time of sampling a majority of fish used in the analysis (i.e.
156 upper mode of size distribution, see below) had a complete smolt appearance (base on the disappearance of
157 parr marks in the skin and silvery coloration, e.g., Debes *et al*, 2020), or were at late stages of smoltification
158 (faint parr marks with close to silvery skin coloration). We excluded a small number of fish in the lower mode to

159 avoid potential interactions associated with this size bimodality (fish fork length < 9 cm, N=69, Supplementary
160 Figure 3). In addition, fish with missing *vgll3* and *six6* genotypes, and sex (N=2, N=12, and N=4, respectively),
161 and a small number of precociously matured males (N=19) were excluded from the analysis. Missing landmarks
162 (0.02% of the total landmarks) were imputed using the *estimate.missing* function in the *geomorph* package
163 (version 4.0.6, Baken *et al*, 2021). A landmarked image was excluded from the analysis if more than one
164 landmark was identified as an outlier in the Procrustes analysis (i.e. > 4 sd away from the mean). These
165 landmarks were not corrected manually, to avoid introducing among technician variation. After data filtering,
166 821 individuals remained in the dataset, of which 731, 737, and 772 individuals were in the small cross section,
167 large cross section, and whole body datasets, respectively (Supplementary Table 1). Within each dataset 16, 18,
168 and 712 individuals were landmarked more than once to estimate repeatability. Landmarking for the first 30
169 and 50 images per researcher for body and cross sections, respectively, were discarded as training sets.

170 *Trait measurements*

171 We quantified variation in 21 traits across various body planes with potential functional significance using the
172 landmark positions (Supplementary Figure 2) and as formulated in Table 1.

173 *Rayed fins and caudal peduncle length:* We measured the length of dorsal, anal, and tail fins, between interior
174 and exterior insertion points, as well as the caudal peduncle (Table 1, Supplementary Figure 2). The variation in
175 these traits may be associated with habitat use, feeding, and swimming performance in salmonids and other
176 fishes (e.g., Jonsson and Jonsson, 2011; Keeley *et al*, 2005). Increased dorsal and pectoral fin sizes in fish are
177 likely important for increased maneuverability and stability, and likely important adaptations for faster flowing
178 streams (Webb, 1984). Specifically, large paired fins (such as pectoral and pelvic fins) in Atlantic salmon are
179 associated with populations that occupy faster flowing and colder streams than slower flowing and warmer
180 rivers, an adaptation attributed to providing effective stability under fast flowing, and turbulent currents
181 (Riddell and Leggett, 1981; Webb, 1988). In Coho salmon, juveniles of interior populations with longer
182 migration distances appear to have smaller fins (Taylor and McPhail, 1985), which may help to reduce drag in
183 long migrations (Varian and Nichols, 2010).

184 *Eye diameter and position, and snout length*: The size of the eye was approximated from the diameter, and the
185 snout length was measured as the distance between the center of the eye and the anterior extreme of the
186 head (Table 1, Supplementary Figure 2). These traits are morphological features associated with trophic
187 specialization and habitat use across fish taxa (Elmer *et al*, 2010; Peris Tamayo *et al*, 2020; Snorrason, 1994).

188 *Aerobic muscle:* We approximate the area of aerobic muscle fibers (also called slow-twitch muscle, or red
189 muscle) by measuring the landmark distances in the cross sections from the lateral line towards the transverse

190 sections, and by measuring the extent of the red muscle along the lateral line (Table 1, Supplementary Figure
191 2). Aerobic muscle provides the energy required during steady, cruise swimming, and helps with thermal
192 acclimation in fishes (Altringham and Ellerby, 1999; Shuman and Coughlin, 2018). Recently, it has been shown
193 that both *vgll3* and *six6* loci are associated with whole body aerobic activity (Prokkola *et al*, 2022), which is a
194 critical physiological process in the salmonid life cycle (Eliason and Farrell, 2015), which may indicate that
195 aerobic muscle mass, as a proxy for aerobic activity, may be associated with these loci.

196 *Cross sectional centroid size and diameter, and vertebral thickness*: We measured cross sectional centroid size
197 and horizontal diameter from both large and small cross section images (Table 1, Supplementary Figure 2), as
198 an approximation for fusiform body shape. A slimmer and more torpedo-shaped body provides improved
199 energy efficiency during cruising and in high flow streams by reducing water drag, and it is an important life
200 history adaptation among fishes (Crossin *et al*, 2004; Jonsson and Jonsson, 2011a; Taylor and McPhail, 1985;
201 Webb, 1988). In contrast, a robust cross section facilitates burst swimming, which is advantageous for prey
202 avoidance and food acquisition (Taylor and McPhail, 1985).

203 We also quantified vertebral width as a proxy for cone diameter, to approximate vertebra's flexibility/stiffness
204 during the lateral bending movement in the undulated motion, which helps to maintain steady swimming at
205 the expense of maneuvering capabilities (Baxter *et al*, 2022; Donatelli *et al*, 2021; Long and Nipper, 1996).

206 *Head and body size:* We quantified head length and width (Table 1, Supplementary Figure 2), which are
207 important determinants of ecotypic divergence via resource and habitat use in fishes (Peris Tamayo *et al*, 2020;
208 Simonsen *et al*, 2017). A larger head and larger snout length may be associated with a feeding regime towards
209 piscivory (Keeley *et al*, 2005), or generally speaking, consuming larger prey items. We also measured head and
210 body centroid sizes as an approximation for the area of the morphometric planes, which is the square root of
211 the sum of squared distances of all the landmarks used in the Procrustes analysis from the point of center of
212 gravity (Klingenberg, 2016). The Atlantic salmon has a smaller head-body ratio compared to the brown trout
213 (Jonsson and Jonsson 2011), which likely makes salmon more efficient swimmers both in strong freshwater
214 currents and during longer marine migrations.

215 *Statistical analysis*

216 Our analysis framework comprised a series of analyses whereby Procrustes shape variables, and morphological
217 traits were used as response variables. These analyses were conducted independently for the body, small cross
218 section, and large cross section. In all analyses, length (centered to zero and scaled to have unit standard
219 deviation), body condition (Fulton's condition factor, scaled), sex, and food treatment were used as covariates.
220 In all models, we implemented genetic variation as additive, where *vgll3* and *six6* genetic effects are coded as

221 0, 1, and 2 for EE, EL, and LL genotypes respectively (E and L refer to the alleles associated with early and late
222 maturation, respectively), so that a unit change in genetic effect represents an additive allelic substitution
223 effect from E to L. Unless otherwise noted, all statistical analyses were performed in R software version 4.4.1 (R
224 Core Team, 2019).

225 We performed multivariate generalized Procrustes analysis to quantify shape variation (Gower, 1975), using
226 the default settings in the *gpagen* function in the geomorph package (version 4.0.8, Baken *et al*, 2021). This
227 function outputs Procrustes shape variables, centered on the mean value for each landmark and normalized for
228 centroid size. Centroid size is the square root of the sum of squared distances of landmarks from the center of
229 gravity (i.e., centroid) and it is highly correlated to the size of the fish.

230 Procrustes shape data was then used to perform a Procrustes linear regression analysis using the *procD.lm*
231 function with default settings (i.e. residual randomization was used for significance testing and type III marginal
232 sums of squares for cross products computations). The model parameters were as follows:

233 $Y = \mu + L + CF + Feed + Tank + Sex + Vgll3 + Six6 + Fam + \varepsilon_{error}$

234 Where Y is the multivariate data frame consisting of x and y coordinates for Procrustes shape coordinates of
235 landmarks, μ is the intercept, L is the scaled fork length, CF is the scaled Fulton's condition factor, and Feed is
236 the factor associated with feed treatment (ad-libitum vs restricted feed). Other terms are the rearing tank ID
237 that the fish were reared after the swim-up stage (Tank), sex (Sex), family (Fam), and the additive genetic
238 effects for *vgll3* and *six6*, respectively. Since the *procD.lm* function does not accommodate random terms, we
239 included tank and family effects as fixed terms. Trait values were averaged prior to the analyses when an
240 individual had replicate measurements. We reported multivariate analysis of variance Pillai's trace statistics,
241 estimated using the *manova.update* function in the RRPP package (version 2.0.3, Collyer *et al*, 2018), and plot
242 individual landmark differences between loci using the *plotRefToTarget* in the geomorph package.

243 To decompose the variation associated with trait values and estimate parameter coefficients, we employed a
244 linear mixed effect (animal) model using the *relmatLmer* function in lme4qtl (version 0.2.2, Ziyatdinov *et al*,
245 2018), which is an implementation of the *lmer* function in the lme4 package (Bates, 2010), and can fit the
246 animal model (i.e., accommodate the additive relatedness matrix). When estimating fixed coefficients, the
247 model was fitted with maximum likelihood using the *REML = FALSE* option in the *relmatLmer* function. The
248 model structure was as follows:

249 $Y = \mu + L + CF + Feed + Sex + Vgll3 + Six6 + \varepsilon_{ID} + \varepsilon_{tank} + \varepsilon_{animal} + \varepsilon_{error}$

Fixed effect terms are as described above except that the fixed tank and family terms in the previous model were replaced with random tank and animal terms, respectively. Random terms thus included, $\varepsilon_{ID}$ which are the individual effects, $\varepsilon_{tank}$ are the effects associated with the tank effects, and $\varepsilon_{error}$ is the measurement error. $\varepsilon_{animal}$ is the random term associated with the background genetic effects after controlling for *vgll3* and *six6* fixed effects. The relatedness matrix was obtained using the pedigree data in Debes *et al* (2019) using the *getA* function in the pedigreem package (version 0.3.4, Vazquez *et al*, 2010). Since we used repeated measurements in the analysis, $\varepsilon_{ID}$ reflects the error term, and $\varepsilon_{error}$ is the residuals that quantifies deviations between repeated samples (i.e. measurement error).

The significance of the fixed effects terms was estimated using the *as_lmerModLmerTest* function in the lmerTest package (version 1.1-3, Kuznetsova *et al*, 2017) in R using type 3 F test with Satterthwaite's method to estimate the effective degrees of freedom.

We then estimated the additive genetic variation, the contribution of *vgll3* and *six6* loci to the additive genetic variation, evolvability, and repeatability. For these, we employed three models similar to above, but the first model ($Model_{VA.full}$) did not contain *vgll3* or *six6* to estimate total additive genetic variation, and was fitted using the *REML = TRUE* option in the *relmatLmer* function to obtain unbiased estimates of variance components. As such, the variance of $\varepsilon_{animal}$ ($V_{animal}$) in the $Model_{VA.full}$ is the total additive genetic variation ($V_A$). Percent contribution of *vgll3* and *six6* are calculated as $\%V_{A.vgll3} = 100 * ( ( 2 \times L_{vgll3} \times E_{vgll3} \times (\beta_{vgll3}^2 - se(\beta)_{vgll3}^2) / V_{animal} )$, and $\%V_{A.six6} = 100 * ( ( 2 \times L_{six6} \times E_{six6} \times (\beta_{six6}^2 - se(\beta)_{six6}^2) ) ) / V_{animal} )$, as in (Luo *et al*, 2003), where $L_{vgll3}$, $E_{vgll3}$, $L_{six6}$ and $E_{six6}$ denotes frequency of L and E alleles in *vgll3* and *six6* loci, respectively, $\beta_{vgll3}$ and $\beta_{six6}$ denotes *six6* and *vgll3* E to L substitution effects, respectively, and se denotes standard error of the estimate. Percent repeatability for each model is calculated as $R = V_{ID} / (V_{ID} + V_{error}) * 100$, and heritability values were calculated as $h^2 = V_{animal} / (V_{animal} + V_{tank} + V_{ID})$, where $V_{tank}$, $V_{ID}$, and $V_{error}$ are the model variance estimates associated with tank ($\varepsilon_{tank}$), individual ($\varepsilon_{ID}$), and error ($\varepsilon_{error}$) terms in $Model_{VA.full}$. Similarly, evolvability ($I_A$) was calculated as $V_A / \bar{y}^2$ using $Model_{VA.full}$, where $\bar{y}$ is the mean trait value (Hansen *et al*, 2011; Houle, 1992). Evolvabilities are interpreted as expected proportional responses in the trait mean under unit selection (i.e. the selection on fitness itself; Hansen *et al*, 2003; Hansen *et al*, 2011). For all variance components, 95% confidence intervals were estimated by obtaining the posterior distributions of random effect terms in the model ($Model_{VA.full}$), using the *sims* function in the arm package(version 1.1.4-4, Gelman and Su, 2020) in R, using 10000 permutations. The simulations generate 10000 estimates for random effect terms, which are then used to calculate the variance components as above, with 250$^{th}$ and 9750$^{th}$ ranked estimates recorded as 95% CIs. We did not control for the effect of dominance in the analyses, which may have inflated the estimates of additive genetic variance (Lynch and Walsh, 1998).

282 ## Results:

283 *Shape analysis:*

284 The multivariate analyses using Procrustes shape variation as the response showed that genetic variation in
285 *six6*, but not in *vgll3*, is associated with shape change in the body plane (Table 2). The change in the body plane
286 appears to be related to changes in the head region associated with *six6*, whereby a substitution from *six6*$^{E}$ to
287 *six6*$^{L}$ elongates the head and slightly bends up the lateral body positioning at ends of the lateral line. In
288 contrast, *vgll3*$^{E}$ to *vgll3*$^{L}$ substitution reduces the head area relative to the body area and pushes the anterior
289 anal fin landmark toward the posterior end of the body plane, albeit the effect is statistically insignificant
290 (Figure 1a). Genetic variation in *vgll3* and *six6* are not associated with overall shape changes in small and large
291 cross sections. Although not statistically significant, a *vgll3*$^{E}$ to *vgll3*$^{L}$ substitution was linked with a narrower
292 horizontal width, a smaller aerobic muscle area in the small cross section (Figure 1b), and a narrower aerobic
293 muscle extension perpendicular to the lateral line in the large cross section (Figure 1c). These results are
294 concordant with the trait-based analysis (see below). Overall, family, tank, feed restriction, and length were
295 important determinants of shape variation in all planes, and condition factor was also significant in the analysis
296 of the body plane (Table 2). Sex was an insignificant determinant of shape in all three body planes (Table 2).

297 *Trait analysis:* After correcting for body length, condition factor, feed restriction, and sex, nine out of 21
298 morphological traits were significantly associated with the *vgll3* locus, while four were associated with *six6*
299 locus (Table 1, Figure 2. See also Supplementary Table 3 for *t*-values and effective degrees of freedoms of
300 terms). In general, the *vgll3*$^{E}$ to *vgll3*$^{L}$ substitution effect decreased trait values (Table 1, Figure 2) with changes
301 in trait values between *vgll3*$^{EE}$ and *vgll3*$^{LL}$ genotypes being > 1%, and up to 3% of the mean trait values (Figure
302 2). Notably, the aerobic muscle depth in the small cross section was reduced by 3.45% ($p < 0.001$) and the
303 aerobic muscle vertical extension in the large cross section was reduced by 2.72% ($p = 0.006$) by the *vgll3*$^{E}$ to
304 *vgll3*$^{L}$ allelic substitution (Table 1, Figure 2). The *vgll3* allelic substitution effect associated with lateral red
305 muscle length was statistically significant when three aerobic muscles trait values were combined into one
306 composite value ($p < 0.001$, Supplementary Table 4). The *vgll3*$^{L}$ allele also decreased vertebral thickness in both
307 small (1.37% decrease, $p = 0.009$) and large (1.21% decrease, $p = 0.032$) cross sections (Table 1, Figure 2). The
308 *vgll3*$^{E}$ to *vgll3*$^{L}$ substitution effect significantly reduced the small cross section diameter by 1.43% ($p = 0.012$),
309 whereas the small section centroid size was reduced by 0.86% ($p = 0.012$, Table 1, Figure 2). Reduced eye
310 diameter, snout length, and anal fin length were also associated with the *vgll3*$^{L}$ allele (Table 1, Figure 2). The
311 trait values for all ray fins (dorsal, anal, pectoral, and tail fins) was trending toward a smaller size in relation to
312 the late maturing genotype (Table 1, Figure 2), and their cumulative effect, i.e., effect size of all trait values

313 combined, was statistically significant ($p$ = 0.022, Supplementary Table 4). We observed that in some traits the
314 variation explained by *vgll3*$^{E}$ to *vgll3*$^{L}$ substitution was up to 50% of the variation explained by length (a factor
315 with strong, positive allometric effect on other trait values, see Table 1), suggesting that this variation is
316 biologically important (Supplementary Figure 4).

317 Most differences explained by variation in the *six6* genomic region were related to changes in head and body
318 size. The *six6*$^{E}$ to *six6*$^{L}$ substitution was associated with a 0.17% decrease in body centroid ($t$ = -3.70, $p$< 0.001)
319 and a 0.47% increase in head centroid size ($t$ = 2.68, $p$ = 0.008, Table 1, Figure 2). The snout length, measured
320 as the distance between the center of the eye and the maximum anterior point in the body, was elongated by
321 0.73% in fish with an additional *six6*$^{L}$ allele ($t$ = 3.05, $p$ = 0.002, Table 1, Figure 2). Head length appears to be a
322 significant determinant of changes in head structure, the effect of an additional *six6*$^{L}$ allele explained a 0.33%
323 increase in average trait value ($t$ = 2.15, $p$ = 0.032, Table 1, Figure 2).

324 Sex effects typically ranged from smaller and up to the same order of magnitude as the allele substitution
325 effects in the life-history loci (Table 1). Notably, the snout, pectoral fin, and anal fin were significantly larger in
326 males compared to females ($p$ = 0.002, $p$ = 0.007, and $p$ = 0.021, respectively. Table 1). In addition, the head
327 centroid was larger in males compared to females ($p$ = 0.040, Table 1). As expected, length was a strong
328 predictor of all traits, and condition factor was also positively associated with most traits (Table 1). Feed
329 restriction was notably associated with a decrease in fin trait values, such as the dorsal fin ($p$ < 0.001), anal fin
330 ($p$ = 0.040), and tail fin ($p$ = 0.003, Table 1). Interestingly, feed restriction substantially reduced the centroid size
331 ($p$ = 0.011), cross section diameter ($p$ = 0.003), and the size of the aerobic muscle ($p$ = 0.005) in the small cross
332 section, but not in the large cross section (Table 1).

333 As length is a strong predictor of both trait values and overall body shape, a spurious association between traits
334 and the life-history loci may be expected if these loci affect trait values via length as a mediator. To test this,
335 we constructed a model to include the interaction between length and life-history loci. Across 21 traits, we did
336 not observe a meaningful difference in main genetic effects, nor were interaction term $t$-values substantial
337 (Supplementary Figure 5), suggesting that length-by-genotype interaction did not drive the estimated relations.

338 *Heritability, evolvability, and additive genetic* variation: Trait heritabilities were low to moderate in most cases,
339 with a mean heritability of 0.19 across all 21 traits (Table 3). Length of tail fin and body centroid size exhibited
340 the highest heritability with 0.50 (95% CI 0.47-0.54) and 0.47 (95% CI 0.43-0.50), followed by the pectoral fin
341 with 0.41 (95% CI 0.36-0.45). The repeatability of trait measurements was moderate (mean repeatability
342 73.0%, Table 3). The relatively low repeatability than expected (Takacs *et al*, 2016) is elevated likely due to low
343 intra-population variation obtained in the common garden setting relative to most morphometrics studies that

344 focuses on larger biological variation, e.g. between ecomorphs of conspecifics or across species, but complex
345 trait measurements combined with suboptimal fish imaging using gutted individuals, and measurer's expertise
346 may also contribute to such variation (Vrdoljak *et al,* 2020, Takacs *et al*, 2016).

347 Evolvabilities (mean-scaled additive genetic variances, denoted as $I_A$) differed greatly among traits (Table 3).
348 Interestingly, body centroid size had the lowest evolvability (<0.001), meaning that even under unit directional
349 selection ( the strength of selection on fitness itself, Hansen *et al,* 2003), the expected increase in this trait
350 value would be less than 0.1%. On the other hand, large cross section aerobic muscle had an evolvability as
351 high as 0.72, meaning that the expected increase in this trait under strong selection could be as high as 71% of
352 the mean trait value. In general, out of 21 traits measured, aerobic muscle and vertebrae thickness traits had
353 higher $I_A$, while centroid sizes and cross section diameters had lower $I_A$ (Table 3).

354 Additive genetic variation explained by the *vgll3* locus was non-zero for 12 traits (Table 3). Consistent with the
355 fixed effect parameterization of the genotype, a substantial portion of the additive genetic variation in vertebra
356 thickness was explained by *vgll3*, with 30.7% and 13.0% for small and large cross sections, respectively (Table
357 3). A significant portion of the additive genetic variation in small section aerobic muscle, cross section
358 diameter, and body centroid was also explained by the *vgll3* locus, with 22.4%, 12.7, and 6.3% for each trait,
359 respectively (Table 3). The contribution of *six6* locus to additive genetic variation associated included snout
360 length (9.4%), and head and body centroid size (5.2% and 4.2%, respectively, Table 3) consistent with the locus
361 effect size.

362

## 363 Discussion

364 Intraspecific differences in functionally important morphological traits may provide important insights into the
365 mechanistic basis of adaptation. We detected several morphological traits in juvenile Atlantic salmon that were
366 linked with variation in genomic regions previously reported to be associated with life-history diversity and
367 known to be under local selection. The genetic polymorphism in the *vgll3* locus appears to shape a suite of
368 traits associated with swimming performance, while the genetic polymorphism in the *six6* locus shapes head
369 and body size, and head features such as snout length, which potentially affects resource acquisition
370 efficiencies for different foraging strategies. On the other hand, these genomic regions have only a small effect
371 on the general shape of the morphological planes. The only statistically significant effect was detected in the
372 body plane plan that was associated with the *six6* loci (Table 2), for which the most striking shape change at the
373 vector level elongates the head length (in relation to $six6^E$ to $six6^L$ substitution, Figure 1), which is concordant

374 with change in the head/body proportions observed in the univariate trait analysis. Our results support these
375 genomic regions having broad phenotypic effects, which may have emerged from either a form of pleiotropy or
376 linkage disequilibrium. Our design does not allow us to categorize the pleiotropic effects further, whether it is
377 based on an effect of single causal variant (biological pleiotropy), or based on effects associated with different
378 phenotypes along a biochemical pathway (mediated pleiotropy), or as a result of linkage disequilibrium
379 between two independent causative loci (spurious pleiotropy, e.g., Solovieff *et al*, 2013). Yet, the strong
380 genetic interdependence among traits associated with *six6* and *vgll3* may have a developmental origin, which is
381 supported by the patterns of gene expression in these genomic regions during development (Moustakas-Verho
382 *et al*, 2020; Kurko *et al*, 2020), and their molecular regulatory functions, (Ahi *et al*, 2022; Kurko *et al*, 2020;
383 Mobley *et al*, 2021;; Verta *et al*, 2020; Verta *et al*, 2024). For example, being a co-transcription factor binding to
384 the TEAD protein, *vgll3* is likely an important regulator of the hippo pathway (Kurko *et al*, 2020) which is
385 involves in organ growth via controlling cell growth (Huang *et al,* 2005). Likewise, allele specific *vgll3* regulation
386 of pubertal development, interact with signaling pathways with diverse molecular functions, such as TGF- β
387 signaling, and wnt pathway which have developmental functions during body axes formation, as well as cell
388 fate commitment (Xue *et al,* 2025; Wu and Hill, 2009).

389 The suite of morphological traits associated with *vgll3* variation reflects changes along a functional axis that
390 facilitates energy-efficient cruising (*vgll3*$^{L}$) versus maneuvering and acceleration (*vgll3*$^{E}$). It appears that that
391 individuals with *vgll3*$^{E}$ genotype have a robust build to facilitate maneuvering and acceleration, and larger
392 aerobic activity (i.e. increased red muscle area, see also below), while individuals with *vgll3*$^{L}$ allele have a
393 slender body build for energy efficiency swimming (i.e. smaller cross section diameter, and smaller ray fins, see
394 also below). Energy efficient cruising is an important trait especially in the marine environment, while better
395 maneuvering and acceleration help coping with biotic (i.e. competition and predation risk) and abiotic (flow
396 regime) factors in the freshwater habitat. The larger aerobic muscle area associated with the *vgll3*$^{E}$ allele could
397 indicate a higher potential for aerobic muscle activity. This result is concordant with (Prokkola *et al*, 2022) who
398 demonstrated that juvenile Atlantic salmon with the early maturing genotype have a higher maximum
399 metabolic rate (MMR) and aerobic scope (AS). Aerobic locomotion is expected to be central for Atlantic salmon
400 during the marine phase, where salmon sub-adults migrate and continuously forage for food. Our results
401 suggest salmon with the early genotype are more likely to maintain sustained swimming and foraging activities,
402 beneficial during marine exploration, which may help to facilitate earlier maturation, with poor performers
403 having to delay reproduction until they can utilize sufficient energy for return migration. On the other hand,
404 having a slender body and energy-efficient cruising may be more advantageous in later years, since individuals
405 with more *vgll3*$^{L}$ alleles appears to perfrom better than indiviauls with *vgll3*$^{E}$ allale at older sea-age groups (i.e.

406 Barson *et al*, 2013). However, it is unclear if the genetic association between life-history loci and morphological
407 traits persists between life stages, or across different environments. The parr-smolt transformation
408 (smoltification) includes morphological changes that prepare juvenile Atlantic salmon for the marine
409 environment (Jonsson and Jonsson, 2011), hence phenotype-genotype association might differ either as a
410 result of smoltification or change in the environment (Aguirre *et al*, 2014). However, since individuals used in
411 this study have a complete or nearly complete smolt phenotype, conclusions may be more relevant to the
412 marine than to the freshwater life stage.

413 Increased vertebral thickness associated with the *vgll3*$^{E}$ allele could provide stiffness for energy efficient
414 undulation movement during steady swimming (Donatelli *et al*, 2021), though it may come at the expense of
415 body flexibility that may facilitate piscivorous prey capture. A larger aerobic muscle area and thicker vertebra
416 may eventually facilitate earlier maturation via more energy efficient resource acquisition at sea, suggesting
417 that local adaptation for optimal age structure could be partly mediated by conditions at sea. Hence, while our
418 results do not explain the causation of early male maturation in freshwater, we cannot explicitly rule out that
419 the link between *vgll3* and age at maturity is mediated via its effect on body shape. Sex was also an important
420 factor shaping the trait variation. Intriguingly, significant changes in shape associated with sex and *vgll3*
421 genotype was also in concordant with respect to maturation timing. As such, males, which on average mature
422 earlier than females, and the *vgll3* allele associated with early maturation had similar direction of change in
423 these morphological traits.

424 Larger fin sizes in fish increase maneuverability and stability (Webb, 1984), and correspondingly in Atlantic
425 salmon, larger fins occur in populations that occupy faster flowing streams (Riddell and Leggett, 1981). Overall,
426 we found that the ray-fins of fish were consistently larger for the *vgll3*$^{E}$ allele than the *vgll3*$^{L}$ allele
427 (Supplementary Table 4). However, this improvement for maneuverability and stability may come at the
428 expense of efficiency in longer marine migrations, as a result of increased drag. For example, in coho salmon,
429 juveniles of inland populations with longer migration distances have smaller fins (Taylor and McPhail, 1985),
430 which may help reduce drag in long migrations (Dynes *et al*, 2005; Varian and Nichols, 2010). A larger cross
431 section diameter and larger fin lengths associated with the *vgll3*$^{E}$ allele likely facilitate maneuvering at the
432 expense of efficient cruising, which is contrast with the *vgll3*$^{E}$ effect that increases aerobic muscle area and
433 vertebral thickness. Similarly, the slender body (a smaller cross section diameter) associated with *vgll3*$^{L}$ is
434 consistent with minimizing drag for a cruising body-form (Webb, 1988), advantageous for a multi-sea winter
435 strategy that migrates longer distances in the ocean (e.g., O'Sullivan *et al*, 2022). On the other hand, the
436 direction of effect on fin size associated with *vgll3*$^{E}$ *to vgll3*$^{L}$ substitution is concordant with the effect of the
437 restricted-food regime, suggesting that the allelic substitution effect may be correlated to food limitation

438 conditions. Thus, overall, the direction of *vgll3* genetic effects is not functionally consistent in relation to
439 proposed ecological roles of these morphological traits.

440 The changes associated with the genetic variation in the *six6* locus that are affecting body and head sizes are
441 linked to ecological processes related to resource acquisition mechanisms. A larger head (and a smaller body)
442 associated with the *six6*$^{L}$ allele and larger snout length may be associated with a feeding regime towards
443 piscivory (Keeley *et al*, 2005), or generally consuming larger prey items. This interpretation corroborates the
444 study by Aykanat *et al* (2020), in which fish with the *six6*$^{LL}$ genotype were shown to be more efficient in
445 resource acquisition than fish with the *six6*$^{EE}$ genotype.

446 Evolvabilities ($I_A$) ranged from normal to very high compared to a recent meta-analysis (Hansen *et al*, 2011).
447 The median evolvability for length traits is 0.001 (or 0.1%, Hansen and Pélabon, 2021; Hansen *et al*, 2011).
448 Normal evolvability values were found for centroid sizes and cross section diameters, while aerobic muscle and
449 vertebrae thickness had high evolvabilities, suggesting that these traits could evolve rapidly in response to
450 selection induced by environmental change. Interestingly, a substantial portion of the additive genetic variation
451 associated with some traits, such as aerobic muscle area and vertebrae thickness, was explained by the *vgll3*
452 locus, suggesting the locus' importance in shaping the additive genetic landscape.

453 Taken together, *vgll3* and *six6* loci have complex associations with morphology. These do not consistently align
454 with adaptive differences between early- and late-maturation genotypes associated with marine migration, but
455 could be important e.g., during spawning where higher maneuverability of smaller males may be beneficial for
456 reproductive success, or in early life stages. On the other hand, it is also plausible that these changes are
457 genetically correlated as part of broad changes during development, and some of which have potentially
458 maladaptive consequences. When traits are genetically correlated, the cumulative adaptive value of trait
459 values cannot be optimal (Schluter, 1996), since breaking suboptimal trait combinations that are genetically
460 correlated may be challenging for evolution (Blows, 2007). Finally, it is challenging to assess the biological
461 significance of the scale of trait variation between loci. However, effect size appears to be large for some trait,
462 i.e., as inferred by up to 50% effect size of allelic substitution effect relative to the effect of length
463 (Supplementary Figure 4), indicating that the genetic variation produces some static allometry between
464 individuals the same cohort, which may have functional and adaptive basis (Pelabon *et al*, 2014).

465 It is important to recognize that extrapolation to the marine stage of Atlantic salmon based on juvenile
466 morphology may have limitations. It is unknown if the genotype-associated morphological variation is
467 correlated between juvenile and adult stages. While there may be genetic correlation between freshwater and
468 marine environments (Fleming *et al*, 1994; Morinville and Rasmussen, 2006; Taylor and McPhail, 1985), the

469 morphological changes associated with adaptation to the marine environment, i.e., the parr-smolt
470 transformation (smoltification), may break apart trait correlations, similar to how metamorphosis takes place
471 in many animal taxa (e.g., Aguirre *et al*, 2014). Since the data in this study were composed of individuals that
472 had completed the parr-smolt transformation, or are close to completion, conclusions are likely more relevant
473 to marine stages than the freshwater stages. However, any adaptive inference associated with a specific life
474 stage should be taken with caution until observed patterns are further tested and verified at different life
475 stages. Finally, while it is reasonable to hypothesize that the observed *vgll3* and *six6* associated morphological
476 variation is adaptively important, the fitness effects of this variation should be better assessed before any
477 evolutionary conclusions can be made (Kingsolver *et al*, 1995).

478 While modelling non-additive architecture within a locus, such as dominance, overdominance, may be
479 relevant, since the *vgll3* locus exhibits sex dependent dominance (Barson *et al*, 2015), in this study, genetic
480 effects were modelled additively, to avoid conceptual and statistical complexities. However, when genetic
481 effects were modelled non-additively (separately for *vgll3* and *six6*), parsimony was meaningfully improved
482 (i.e., AIC for dominance gene effect model was 2 units smaller than the AIC for additive gene effect model) for
483 four out of 21 traits for the *vgll3* gene, while none of the non-additive models performed better than additive
484 models for the *six6* gene (Supplementary Figure 6a). In all three traits with significant non-additive genetic
485 effect, a dominance model with *vgll3*$^{EL}$ effect resembling *vgll3*$^{LL}$ was supported (Supplementary Figure 6 b-d),
486 suggesting a possible role of dominance shaping some of the trait values.

487 In conclusion, we have detected substantial morphological variation associated with two genomic regions,
488 which are also major determinants of life-history variation and known to be under local selection. These loci
489 appear to influence multiple, strongly correlated traits, suggestive of a broad regulatory role with impacts
490 across the whole life cycle. How these genetic correlations are shaped – via single locus pleiotropy or close
491 physical linkage of multiple genes – remains to be determined.

492

## 493 Acknowledgment

494 We thank Artur Porto for discussion related to morphometric analyses, and Seija Tillanen, Jacqueline E.
495 Moustakas-Verho, Nikolai Piavchenko for helps with sampling. This work was supported by the Research
496 Council of Finland (grant nos. 328860, 353388, and 325964 to TA, and 314254, 327255 and 342851 to CRP), and
497 the European Research Council under the European Articles Union's Horizon 2020 and Horizon Europe research
498 and innovation programs (grant no. 742312 and 101054307 to CRP). Views and opinions expressed are

however those of the author(s) only and do not necessarily reflect those of the European Union or the European Research Council Executive Agency. Neither the European Union nor the granting authority can be held responsible for them. LG was supported by Erasmus+ programme. The authors declare no competing interests.

## Ethical approval

The experiments were approved by the Project Authorisation Board (ELLA) on behalf of the Regional Administrative Agency for Southern Finland (ESAVI) under experimental license ESAVI/2778/2018.

## Author contributions

TA, VLP, and GHB conceptualized the paper. TA analyzed the data with significant input from GHB and PVD. SJ and LG performed landmarking. AHH and AR prepared and scanned the cross sections. JE, and CRP oversaw the resources and infrastructure. PVD and CRP devised the breeding design and reared the fish. TA and PVD sampled the fish and digitized the images. TA drafted the MS with significant inputs from PVD, VLP, and GHB, and all coauthors contributed to subsequent drafts.

## Conflict of Interest

The authors declare no competing interests.

## References:

Aguirre JD, Blows MW, Marshall DJ (2014). The genetic covariance between life cycle stages separated by metamorphosis. *Proceedings Biological sciences / The Royal Society* **281**(1788)**:** 20141091.

Ahi EP, Sinclair-Waters M, Moustakas-Verho J, Jansouz S, Primmer CR (2022). Strong regulatory effects of *vgll3* genotype on reproductive axis gene expression in juvenile male Atlantic salmon. *General and Comparative Endocrinology* **325:** 114055.

Altringham JD, Ellerby DJ (1999). Fish swimming: Patterns in muscle function. *Journal of Experimental Biology* **202**(Pt 23)**:** 3397-3403.

Archambeault SL, Bartschi LR, Merminod AD, Peichel CL (2020). Adaptation via pleiotropy and linkage: Association mapping reveals a complex genetic architecture within the stickleback *Eda* locus. *Evolution Letters* **4**(4)**:** 282-301.

Asheim ER, Debes PV, House A, Liljestrom P, Niemela PT, Siren JP *et al* (2023). Atlantic salmon (*Salmo salar*) age at maturity is strongly affected by temperature, population and age-at-maturity genotype. *Conservation Physiology* **11**(1)**:** coac086.

Aykanat T, McLennan D, Metcalfe NB, Prokkola JM (2024). Early survival in Atlantic salmon is associated with parental genotypes at loci linked to timing of maturation. *Evolution* **78**(8)**:** 1441-1452.

Aykanat T, Ozerov M, Vaha JP, Orell P, Niemela E, Erkinaro J *et al* (2019). Co-inheritance of sea age at maturity and iteroparity in the Atlantic salmon *vgll3* genomic region. *Journal of Evolutionary Biology* **32**(4)**:** 343-355.

Aykanat T, Rasmussen M, Ozerov M, Niemela E, Paulin L, Vaha JP *et al* (2020). Life-history genomic regions explain differences in Atlantic salmon marine diet specialization. *Journal of Animal Ecology* **89**(11)**:** 2677-2691.

Ayllon F, Kjaerner-Semb E, Furmanek T, Wennevik V, Solberg MF, Dahle G *et al* (2015). The *vgll3* locus controls age at maturity in wild and domesticated Atlantic salmon (*Salmo salar* L.) Males. *PLoS Genet* **11**(11)**:** e1005628.

Baken EK, Collyer ML, Kaliontzopoulou A, Adams DC (2021). geomorph v4.0 and gmShiny: Enhanced analytics and a new graphical interface for a comprehensive morphometric experience. *Methods in Ecology and Evolution* **12**(12)**:** 2355-2363.

Bangura PB, Tiira K, Niemela PT, Erkinaro J, Liljestrom P, Toikkanen A *et al* (2022). Linking *vgll3* genotype and aggressive behaviour in juvenile Atlantic salmon (*Salmo salar*). *Journal Fish Biology* **100**(5)**:** 1264-1271.

Barrett RD, Hoekstra HE (2011). Molecular spandrels: tests of adaptation at the genetic level. *Nature Reviews Genetics* **12**(11)**:** 767-780.

Barson NJ, Aykanat T, Hindar K, Baranski M, Bolstad GH, Fiske P *et al* (2015). Sex-dependent dominance at a single locus maintains variation in age at maturity in salmon. *Nature* **528**(7582)**:** 405-408.

Bates DM (2010). lme4: Mixed-effects modeling with R.

Baxter D, Cohen KE, Donatelli CM, Tytell ED (2022). Internal vertebral morphology of bony fishes matches the mechanical demands of different environments. *Ecology and evolution* **12**(11)**:** e9499.

Blows MW (2007). A tale of two matrices: multivariate approaches in evolutionary biology. *Journal of Evolutionary Biology* **20**(1)**:** 1-8.

Boyle EA, Li YI, Pritchard JK (2017). An expanded view of complex traits: From polygenic to omnigenic. *Cell* **169**(7)**:** 1177-1186.

Chan YF, Marks ME, Jones FC, Villarreal G, Jr., Shapiro MD, Brady SD *et al* (2010). Adaptive evolution of pelvic reduction in sticklebacks by recurrent deletion of a *Pitx1* enhancer. *Science* **327**(5963)**:** 302-305.

Collyer ML, Adams DC, Freckleton R (2018). RRPP: An R package for fitting linear models to high-dimensional data using residual randomization. *Methods in Ecology and Evolution* **9**(7)**:** 1772-1779.

Colosimo PF, Hosemann KE, Balabhadra S, Villarreal G, Jr., Dickson M, Grimwood J *et al* (2005). Widespread parallel evolution in sticklebacks by repeated fixation of Ectodysplasin alleles. *Science* **307**(5717)**:** 1928-1933.

Crossin GT, Hinch SG, Farrell AP, Higgs DA, Lotto AG, Oakes JD *et al* (2004). Energetics and morphology of sockeye salmon: effects of upriver migratory distance and elevation. *Journal Fish Biology* **65**(3)**:** 788-810.

Debes PV, Piavchenko N, Erkinaro J, Primmer CR (2020). Genetic growth potential, rather than phenotypic size, predicts migration phenotype in Atlantic salmon. *Proceedings Biological sciences / The Royal Society* **287**(1931)**:** 20200867.

Debes PV, Piavchenko N, Ruokolainen A, Ovaskainen O, Moustakas-Verho JE, Parre N *et al* (2019). Large single-locus effects for maturation timing are mediated via condition variation in Atlantic salmon. *bioRxiv***:** 780437 (v780433).

Debes PV, Piavchenko N, Ruokolainen A, Ovaskainen O, Moustakas-Verho JE, Parre N *et al* (2021). Polygenic and major-locus contributions to sexual maturation timing in Atlantic salmon. *Molecular Ecology* **30**(18)**:** 4505-4519.

Donatelli CM, Roberts AS, Scott E, DeSmith K, Summers D, Abu-Bader L *et al* (2021). Foretelling the flex-vertebral shape predicts behavior and ecology of fishes. *Integrative and Comparative Biology* **61**(2)**:** 414-426.

Dynes J, Magnan P, Bernatchez L, Rodríguez MA (2005). Genetic and morphological variation between two forms of lacustrine brook charr. *Journal Fish Biology* **54**(5)**:** 955-972.

Eliason EJ, Farrell AP (2015). Oxygen uptake in Pacific salmon *Oncorhynchus* spp.: when ecology and physiology meet. *Journal Fish Biology*.

Elmer KR, Kusche H, Lehtonen TK, Meyer A (2010). Local variation and parallel evolution: morphological and genetic diversity across a species complex of neotropical crater lake cichlid fishes. *Philosophical transactions of the Royal Society of London Series B, Biological sciences* **365**(1547)**:** 1763-1782.

610 Endler JA (2000). Adaptive genetic variation in the wild. In: Mousseau TA, SinerVo B and Endler JA (eds)
611 *Adaptive Genetic Variation in the Wild*. Oxford University Press.

612

613 Ferry-Graham LA, Bolnick DI, Wainwright PC (2002). Using functional morphology to examine the ecology and
614 evolution of specialization. *Integrative and Comparative Biology* **42**(2)**:** 265-277.

615

616 Fitzgerald DB, Winemiller KO, Sabaj Pérez MH, Sousa LM, Seymour C (2017). Using trophic structure to reveal
617 patterns of trait-based community assembly across niche dimensions. *Functional Ecology* **31**(5)**:** 1135-1144.

618

619 Fleming IA, Jonsson B, Gross MR (1994). Phenotypic divergence of sea-ranched, farmed, and wild salmon.
620 *Canadian Journal of Fisheries and Aquatic Sciences* **51**(12)**:** 2808-2824.

621

622 Gelman A, Su YS (2020). arm: Data analysis using regression and multilevel/hierarchical models. R package
623 version 1.11-2.

624

625 Gower JC (1975). Generalized procrustes analysis. *Psychometrika* **40**(1)**:** 33-51.

626

627 Hansen TF, Pélabon C (2021). Evolvability: A quantitative-genetics perspective. *Annual Review of Ecology,*
628 *Evolution, and Systematics* **52**(1)**:** 153-175.

629

630 Hansen TF, Pelabon C, Armbruster WS, Carlson ML (2003). Evolvability and genetic constraint in *Dalechampia*
631 blossoms: components of variance and measures of evolvability. *Journal of Evolutionary Biology* **16**(4)**:** 754-
632 766.

633

634 Hansen TF, Pélabon C, Houle D (2011). Heritability is not evolvability. *Evolutionary Biology* **38**(3)**:** 258-277.

635

636 Hoar WS (1988). 4 The physiology of smolting salmonids. In: Hoar WS and Randall DJ (eds) *Fish Physiology*.
637 Academic Press. Vol. 11, pp 275-343.

638

639 Houle D (1992). Comparing evolvability and variability of quantitative traits. *Genetics* **130:** 195-204.

640

641 Huang, J, Wu S, Barrera J, Matthews K, Pan D (2005). The Hippo signaling pathway coordinately regulates cell
642 proliferation and apoptosis by inactivating Yorkie, the Drosophila Homolog of YAP. *Cell* **122**, 421-434.

643

644 Jakobson CM, Jarosz DF (2020). What has a century of quantitative genetics taught us about nature's genetic
645 tool kit? *Annual Review of Genetics* **54:** 439-464.

646

647 Jimenez-Gomez JM, Wallace AD, Maloof JN (2010). Network analysis identifies *ELF3* as a QTL for the shade
648 avoidance response in Arabidopsis. *PLoS Genetics* **6**(9)**:** e1001100.

649

Jones, F.C., Grabherr, M.G., Chan, Y.F., Russell, P., Mauceli, E., Johnson, J. et al. (2012). The genomic basis of adaptive evolution in threespine sticklebacks. Nature 484, 55-61.

Jonsson B, Jonsson N (2011). *Ecology of Atlantic salmon and brown trout : habitat as a template for life histories*. Springer: Dordrecht.

Kawecki TJ, Ebert D (2004). Conceptual issues in local adaptation. *Ecology Letters* **7**(12)**:** 1225-1241.

Keeley ER, Parkinson EA, Taylor EB (2005). Ecotypic differentiation of native rainbow trout (*Oncorhynchus mykiss*) populations from British Columbia. *Canadian Journal of Fisheries and Aquatic Sciences* **62**(7)**:** 1523-1539.

Kern EMA, Robinson D, Gass E, Godwin J, Langerhans RB (2016). Correlated evolution of personality, morphology and performance. *Animal Behaviour* **117**, 79-86.

King DE (2009). Dlib-Ml: A machine learning toolkit. *Journal of Machine Learning Research* **10** (Jul), 1755–1758.

Kingsolver JG, Woods HA, Gilchrist G (1995). Traits related to fitness. *Science* **267**(5196)**:** 396.

Klingenberg CP (2016). Size, shape, and form: concepts of allometry in geometric morphometrics. *Development Genes and Evolution* **226**(3)**:** 113-137.

Kurko J, Debes PV, House AH, Aykanat T, Erkinaro J, Primmer CR (2020). Transcription profiles of age-at-maturity-associated genes suggest cell fate commitment regulation as a key factor in the Atlantic salmon Maturation Process. *G3* **10**(1)**:** 235-246.

Kuznetsova A, Brockhoff PB, Christensen RHB (2017). lmerTest package: Tests in linear mixed effects models. *Journal of Statistical Software* **82**(13).

Long JH, Nipper KS (1996). The importance of body stiffness in undulatory propulsion. *American Zoologist* **36**(6)**:** 678-694.

Lundsgaard-Hansen B, Matthews B, Vonlanthen P, Taverna A, Seehausen O (2013). Adaptive plasticity and genetic divergence in feeding efficiency during parallel adaptive radiation of whitefish (*Coregonus* spp.). *Journal of Evolutionary Biology* **26**(3)**:** 483-498.

Luo L, Mao Y, Xu S (2003). Correcting the bias in estimation of genetic variances contributed by individual QTL. *Genetica* **119**(2)**:** 107-113.

Lynch M, Walsh B (1998). *Genetics and analysis of quantitative traits*. Sinauer Associates: Sunderland, MA.

690
691 Mackay TF, Stone EA, Ayroles JF (2009). The genetics of quantitative traits: challenges and prospects. *Nature*
692 *Reviews Genetics* **10**(8)**:** 565-577.

693
694 Miettinen A, Dannewitz J, Palm S, Ahi EP, Romakkaniemi A, Vähä V *et al* (2023). Loci associated with
695 maturation, migration and appetite control are linked with signals of fine-scale local selection in a large Atlantic
696 salmon population. *bioRxiv***:** 2023.2008.2023.553800.

697
698 Mindel BL, Neat FC, Trueman CN, Webb TJ, Blanchard JL (2016). Functional, size and taxonomic diversity of fish
699 along a depth gradient in the deep sea. *PeerJ* **4:** e2387.

700
701 Mobley KB, Aykanat T, Czorlich Y, House A, Kurko J, Miettinen A *et al* (2021). Maturation in Atlantic salmon
702 (*Salmo salar*, Salmonidae): a synthesis of ecological, genetic, and molecular processes. *Reviews in Fish Biology*
703 *and Fisheries* **31**(3)**:** 523-571.

704
705 Morinville GR, Rasmussen JB (2006). Does life-history variability in salmonids affect habitat use by juveniles? A
706 comparison among streams open and closed to anadromy. *Journal of Animal Ecology* **75**(3)**:** 693-704.

707
708 Morinville GR, Rasmussen JB (2007). Distinguishing between juvenile anadromous and resident brook trout
709 (*Salvelinus fontinalis*) using morphology. *Environmental Biology of Fishes* **81**(2)**:** 171-184.

710
711 Moustakas-Verho JE, Kurko J, House AH, Erkinaro J, Debes P, Primmer CR (2020). Developmental expression
712 patterns of six6: A gene linked with spawning ecotypes in Atlantic salmon. *Gene Expression Patterns* **38:**
713 119149.

714
715 Nielsen EE, Hemmer-Hansen J, Larsen PF, Bekkevold D (2009). Population genomics of marine fishes:
716 identifying adaptive variation in space and time. *Molecular Ecology* **18**(15)**:** 3128-3150.

717
718 O'Sullivan RJ, Ozerov M, Bolstad GH, Gilbey J, Jacobsen JA, Erkinaro J *et al* (2022). Genetic stock identification
719 reveals greater use of an oceanic feeding ground around the Faroe Islands by multi-sea winter Atlantic salmon,
720 with variation in use across reporting groups. *ICES Journal of Marine Science* **79**(9)**:** 2442-2452.

721
722 Olson-Manning CF, Wagner MR, Mitchell-Olds T (2012). Adaptive evolution: evaluating empirical support for
723 theoretical predictions. *Nature Reviews Genetics* **13**(12)**:** 867-877.

724
725 Orr HA (2000). Adaptation and the cost of complexity. *Evolution* **54**(1)**:** 13-20.

726
727 Otto SP (2004). Two steps forward, one step back: the pleiotropic effects of favoured alleles. *Proceedings*
728 *Biological sciences / The Royal Society* **271**(1540)**:** 705-714.

729
730 Paaby AB, Rockman MV (2013). The many faces of pleiotropy. *Trends in Genetics* **29**(2)**:** 66-73.

Pelabon C, Firmat C, Bolstad GH, Voje KL, Houle D, Cassara J et al (2014). Evolution of morphological allometry. *Annals of the New York Academy of Sciences* **1320**, 58-75.

Peris Tamayo AM, Devineau O, Praebel K, Kahilainen KK, Ostbye K (2020). A brain and a head for a different habitat: Size variation in four morphs of Arctic charr (*Salvelinus alpinus* (L.)) in a deep oligotrophic lake. *Ecology and evolution* **10**(20)**:** 11335-11351.

Pritchard VL, Makinen H, Vaha JP, Erkinaro J, Orell P, Primmer CR (2018). Genomic signatures of fine-scale local selection in Atlantic salmon suggest involvement of sexual maturation, energy homeostasis and immune defence-related genes. *Molecular Ecology* **27**(11)**:** 2560-2575.

Prokkola JM, Asheim ER, Morozov S, Bangura P, Erkinaro J, Ruokolainen A *et al* (2022). Genetic coupling of life-history and aerobic performance in Atlantic salmon. *Proceedings Biological sciences / The Royal Society* **289**(1967)**:** 20212500.

Proulx R, Magnan P (2004). Contribution of phenotypic plasticity and heredity to the trophic polymorphism of lacustrine brook charr (Salvelinus fontinalis M.). *Evolutionary Ecology Research* **6**(4)**:** 503-522.

R Core Team. (2019). R Foundation for Statistical Computing, Vienna, Austria.

Riddell BE, Leggett WC (1981). Evidence of an adaptive basis for geographic-variation in body morphology and time of downstream migration of juvenile Atlantic salmon (*Salmo salar*). *Canadian Journal of Fisheries and Aquatic Sciences* **38**(3)**:** 308-320.

Schluter D (1996). Ecological Causes of Adaptive Radiation. *American Naturalist*

Shapiro MD, Marks ME, Peichel CL, Blackman BK, Nereng KS, Jonsson B, *et al* (2004). Genetic and developmental basis of evolutionary pelvic reduction in threespine sticklebacks. *Nature* **428**, 717-723.

Shuman JL, Coughlin DJ (2018). Red muscle function and thermal acclimation to cold in rainbow smelt, *Osmerus mordax*, and rainbow trout, *Oncorhynchus mykiss*. *Journal of Experimental Zoology Part A: Ecological and Integrative Physiology* **329**(10)**:** 547-556.

Simonsen MK, Siwertsson A, Adams CE, Amundsen PA, Praebel K, Knudsen R (2017). Allometric trajectories of body and head morphology in three sympatric Arctic charr (*Salvelinus alpinus* (L.)) morphs. *Ecology and evolution* **7**(18)**:** 7277-7289.

Sinclair-Waters M, Odegard J, Korsvoll SA, Moen T, Lien S, Primmer CR *et al* (2020). Beyond large-effect loci: large-scale GWAS reveals a mixed large-effect and polygenic architecture for age at maturity of Atlantic salmon. *Genetics Selection Evolution* **52**(1)**:** 9.

Snorrason S (1994). Trophic specialization in Arctic charr *Salvelinus alpinus* (Pisces; Salmonidae): morphological divergence and ontogenetic niche shifts. *Biological Journal of the Linnean Society* **52**(1)**:** 1-18.

Solovieff N, Cotsapas C, Lee PH, Purcell SM, Smoller JW (2013). Pleiotropy in complex traits: challenges and strategies. *Nature Reviews Genetics* **14**(7)**:** 483-495.

Svanbäck R, Eklöv P (2003). Morphology dependent foraging efficiency in perch: a trade-off for ecological specialization? *Oikos* **102**(2)**:** 273-284.

Takacs P, Vital Z, Ferincz A, Staszny A (2016). Repeatability, reproducibility, separative power and subjectivity of different fish morphometric analysis methods. *PLoS One* **11**, e0157890.

Taylor EB, McPhail JD (1985). Variation in body morphology among British Columbia populations of coho salmon, *Oncorhynchus kisutch*. *Canadian Journal of Fisheries and Aquatic Sciences* **42**(12)**:** 2020-2028.

Varian A, Nichols KM (2010). Heritability of morphology in brook trout with variable life histories. *PLoS One* **5**(9)**:** e12950.

Vazquez AI, Bates DM, Rosa GJ, Gianola D, Weigel KA (2010). Technical note: an R package for fitting generalized linear mixed models in animal breeding. *Journal of Animal Science***88**(2)**:** 497-504.

Verta JP, Debes PV, Piavchenko N, Ruokolainen A, Ovaskainen O, Moustakas-Verho JE *et al* (2020). Cis-regulatory differences in isoform expression associate with life history strategy variation in Atlantic salmon. *PLoS Genetics* **16**(9)**:** e1009055.

Verta JP, Moustakas-Verho JE, Donner I, Frapin M, Ruokolainen A, Debes PV *et al* (2024). A complex mechanism translating variation of a simple genetic architecture into alternative life histories. *Proceedings of the National Academy of Sciences of the USA* **121**(48)**:** e2402386121.

Vrdoljak J, Sanchez KI, Arreola-Ramos R, Diaz Huesa EG, Villagra A, Avila LJ *et al* (2020). Testing repeatability, measurement error and species differentiation when using geometric morphometrics on complex shapes: a case study of Patagonian lizards of the genus *Liolaemus* (Squamata: Liolaemini). *Biological Journal of the Linnean Society* **130**, 800-812.

Wagner GP, Altenberg L (1996). Perspective: Complex adaptations and the evolution of evolvability. *Evolution* **50**(3)**:** 967-976.

Wagner GP, Zhang J (2011). The pleiotropic structure of the genotype-phenotype map: the evolvability of complex organisms. *Nature Reviews Genetics* **12**(3)**:** 204-213.

Webb PW (1984). Body form, locomotion and foraging in aquatic vertebrates. *American Zoologist* **24**(1)**:** 107-120.

813
814 Webb PW (1988). Simple physical principles and vertebrate aquatic locomotion. *American Zoologist* **28**(2)**:** 709-
815 725.

816
817 Weith M, Grossbach J, Clement-Ziza M, Gillet L, Rodriguez-Lopez M, Marguerat S *et al* (2023). Genetic effects
818 on molecular network states explain complex traits. *Molecular Systems Biology* **19**(8)**:** e11493.

819
820 Wu MY, Hill CS (2009). *Tgf-beta* superfamily signaling in embryonic development and homeostasis.
821 *Developmental Cell* **16**, 329-343.
822 Xue C, Chu Q, Shi Q, Zeng Y, Lu J, Li L (2025). Wnt signaling pathways in biology and disease: mechanisms and
823 therapeutic advances. *Signal Transduction and Targeted Therapy* **10**, 106.

824
825 Ziyatdinov A, Vazquez-Santiago M, Brunel H, Martinez-Perez A, Aschard H, Soria JM (2018). lme4qtl: linear
826 mixed models with flexible covariance structure for genetic studies of related individuals. *BMC Bioinformatics*
827 **19**(1)**:** 68.

828
829 Zueva KJ, Lumme J, Veselov AE, Primmer CR, Pritchard VL (2020). Population genomics reveals repeated signals
830 of adaptive divergence in the Atlantic salmon of north-eastern Europe. *Journal of Evolutionary Biology* **34**(6)**:**
831 866-878.

## Tables (3) and Figures (2):

**Table 1:** Estimated fixed effect coefficients for 21 morphological traits obtained across three body planes. Trait lengths are given in centimeters (cm) for all traits. Coef. (SE) indicates coefficients and their standard error. B, S, and L in the body plane column indicates lateral view of the body, small and large cross sections, respectively. Significant *p* values are indicated with asterisk (* and ** denotes *p*<0.05 and *p*<0.01, respectively).

| Trait | Body Plane[1] | Trait value formula[1] | Intercept | Length (scaled) | | Condition factor (scaled) | | Feed restriction (*ad libitum* to restricted) | | Sex (female to male) | | vgll3 (E to L) | | six6 (E to L) | |
|---|---|---|---|---|---|---|---|---|---|---|---|---|---|---|---|
| | | | coef. (SE) | coef. (SE) | *p* value | coef. (SE) | *p* value | coef. (SE) | *p* value | coef. (SE) | *p* value | coef. (SE) | *p* value | coef. (SE) | *p* value |
| Dorsal fin | B | B [12:13] | 2.0439 (0.0305) | 0.1560 (0.0064) | <0.001** | -0.0016 (0.0041) | 0.696 | -0.1222 (0.0176) | <0.001** | 0.0228 (0.0124) | 0.067 | -0.0246 (0.0148) | 0.106 | -0.0142 (0.0126) | 0.263 |
| Anal fin | B | B [16:17] | 1.35902 (0.0164) | 0.06636 (0.0041) | <0.001** | 0.00043 (0.0038) | 0.909 | -0.02549 (0.0094) | 0.0402* | 0.01759 (0.0076) | 0.021* | -0.01979 (0.0077) | 0.017* | 0.00658 (0.0075) | 0.378 |
| Pectoral fin | B | B [10:11] | 2.0973 (0.0202) | 0.1148 (0.0029) | <0.001** | 0.0082 (0.0022) | <0.001** | -0.0376 (0.0151) | 0.059 | 0.0143 (0.0053) | 0.007** | -0.0102 (0.0096) | 0.29 | 0.0030 (0.0058) | 0.601 |
| Tail fin | B | B [19:20] | 8.3e-01 (0.0098) | 4.1e-02 (0.0015) | <0.001** | -8.2e-03 (0.0013) | <0.001** | -2.1e-02 (0.0037) | 0.003** | 2.8e-05 (0.0027) | 0.992 | -4.0e-03 (0.0051) | 0.432 | 3.1e-03 (0.0030) | 0.292 |
| Caudal peduncle | B | B [15:18] | 8.7e-01 (0.00428) | 6.0e-02 (0.00078) | <0.001** | 1.1e-02 (0.00071) | <0.001** | 1.3e-03 (0.00198) | 0.529 | 2.3e-03 (0.00144) | 0.118 | -2.3e-03 (0.00219) | 0.294 | -6.7e-05 (0.00153) | 0.965 |
| Vertebra thickness | Sml | S [3:4] | 2.4e-01 (0.00265) | 1.6e-02 (0.00081) | <0.001** | 1.8e-03 (0.00082) | 0.0241* | 2.3e-03 (0.00165) | 0.172 | -2.2e-03 (0.00157) | 0.168 | -3.3e-03 (0.00117) | 0.009** | 5.3e-05 (0.00138) | 0.969 |
| Vertebra thickness | Lrg | L [6:7] | 0.25170 (0.00282) | 0.01394 (0.00077) | <0.001** | 0.00467 (0.00078) | <0.001** | -0.00238 (0.00155) | 0.125 | -0.00244 (0.00146) | 0.096 | -0.00297 (0.00131) | 0.032* | 0.00023 (0.00137) | 0.866 |
| Cross section diameter | Sml | S [5:7] | 1.1423 (0.0136) | 0.0753 (0.0027) | <0.001** | 0.0134 (0.0027) | <0.001** | -0.0562 (0.0114) | 0.003** | 0.0020 (0.0049) | 0.683 | -0.0157 (0.0058) | 0.012* | -0.0054 (0.0050) | 0.279 |
| Cross section diameter | Lrg | L [12:8] | 2.0269 (0.0117) | 0.1477 (0.0021) | <0.001** | 0.0312 (0.0021) | <0.001** | 0.0050 (0.0108) | 0.666 | 0.0019 (0.0039) | 0.621 | -0.0047 (0.0048) | 0.335 | -0.0046 (0.0039) | 0.248 |
| Aerobic muscle | Sml | S [(7:8+5:6)/2] | 0.17549 (0.00353) | 0.01024 (0.00082) | <0.001** | 0.00137 (0.00083) | 0.0981 | -0.01237 (0.00290) | 0.0051** | 0.00056 (0.00153) | 0.715 | -0.00557 (0.00148) | <0.001** | -0.00210 (0.00149) | 0.159 |
| Aerobic muscle | Lrg | L [(8:9+12:13)/2) | 0.2349 (0.00408) | 0.0185 (0.00094) | <0.001** | 0.0033 (0.00094) | <0.001** | 0.0070 (0.00239) | 0.025* | 0.0017 (0.00175) | 0.34 | -0.0024 (0.00195) | 0.222 | -0.0022 (0.00174) | 0.198 |
| Aerobic muscle vertical extension | Lrg | L [(14:15+10:11)/2] | 0.879 (0.0198) | 0.087 (0.0039) | <0.001** | 0.026 (0.0039) | <0.001** | 0.038 (0.0176) | 0.0916 | -0.012 (0.0073) | 0.089 | -0.024 (0.0081) | 0.006** | 0.013 (0.0072) | 0.067 |
| Eye diameter[2] | B | B [(2:3+4+5)/2] | 5.5e-01 (0.00358) | 2.2e-02 (0.00094) | <0.001** | 3.3e-04 (0.00092) | 0.723 | 1.8e-03 (0.00285) | 0.546 | -1.7e-06 (0.00175) | 0.999 | -3.2e-03 (0.00152) | 0.055 | 2.6e-03 (0.00163) | 0.112 |
| Snout length | B | B [1:0] | 0.78061 (0.00458) | 0.03839 (0.00097) | <0.001** | -0.00054 (0.00083) | 0.509 | -0.00277 (0.00196) | 0.157 | 0.00557 (0.00183) | 0.002** | -0.00607 (0.00232) | 0.013* | 0.00575 (0.00189) | 0.002** |
| Eye vertical position | B | B [0:6] | 0.40996 (0.0052) | 0.02487 (0.0012) | <0.001** | 0.00460 (0.0010) | <0.001** | 0.00934 (0.0036) | 0.0538 | 0.00024 (0.0022) | 0.912 | -0.00031 (0.0024) | 0.899 | 0.00057 (0.0022) | 0.794 |
| Head length[3] | B | B [1:7] | 2.1453 (0.0232) | 0.1347 (0.0034) | <0.001** | 0.0074 (0.0025) | 0.0034* | -0.0370 (0.0224) | 0.162 | 0.0106 (0.0064) | 0.094 | -0.0074 (0.0098) | 0.455 | 0.0146 (0.0068) | 0.032* |
| Head width[3] | B | B [8:9] | 1.59855 (0.0052) | 0.09654 (0.0015) | <0.001** | 0.01633 (0.0013) | <0.001** | 0.02432 (0.0030) | <0.001** | 0.00420 (0.0028) | 0.13 | -0.00046 (0.0024) | 0.85 | 0.00030 (0.0026) | 0.907 |
| Body centroid size | B | From Procrustes analysis | 13.1556 (0.0201) | 0.9084 (0.0031) | <0.001** | 0.0090 (0.0026) | <0.001** | 0.0505 (0.0124) | 0.0118* | -0.0088 (0.0057) | 0.124 | 0.0253 (0.0099) | 0.014* | -0.0227 (0.0061) | <0.001** |
| Head centroid size | B | From Procrustes analysis | 2.2095 (0.0131) | 0.1312 (0.0020) | <0.001** | 0.0143 (0.0016) | <0.001** | -0.0073 (0.0144) | 0.632 | 0.0077 (0.0037) | 0.040* | -0.0075 (0.0050) | 0.148 | 0.0104 (0.0039) | 0.008** |
| Centroid size | Sml | From Procrustes analysis | 1.4166 (0.0129) | 0.0968 (0.0023) | <0.001** | 0.0199 (0.0023) | <0.001** | -0.0387 (0.0102) | 0.0111* | 0.0033 (0.0042) | 0.432 | -0.0119 (0.0058) | 0.048* | -0.0048 (0.0044) | 0.28 |
| Centroid size | Lrg | From Procrustes analysis | 3.5944 (0.0177) | 0.2598 (0.0029) | <0.001** | 0.0601 (0.0029) | <0.001** | 0.0202 (0.0133) | 0.209 | -0.0015 (0.0053) | 0.778 | -0.0097 (0.0082) | 0.244 | -0.0054 (0.0056) | 0.337 |

1: The trait values are based on landmarks as numbered and indicated in Supplementary Figure 2.
2: Eye origin is the center point of eye landmarks, and calculated using landmarks 2, 3, 4, and 5, which are the anterior, posterior, dorsal and ventral extremes of the bony orbit of the eye.
3: Landmark 7 is the posterior point of the bony operculum. Landmarks 8 and 9 are the points of maximum curvature of the bony operculum at the ventral and dorsal ends, respectively.

**Table 2:** Multivariate analysis using Procrustes shape variable across three body planes in juvenile Atlantic salmon. Pillai is the Pillai's trace test statistic to evaluate each term's significance in the multivariate analysis of variance.

| Terms | Large cross section | | | | Small cross section | | | | Body | | | |
|---|---|---|---|---|---|---|---|---|---|---|---|---|
| | df | Pillai | *z* value | *p* value | df | Pillai | *z* value | *p* value | df | Pillai | *z* value | *p* value |
| **Length (scaled)** | 1 | 0.207 | 8.231 | 0.001 | 1 | 0.042 | 2.574 | 0.008 | 1 | 0.530 | 15.369 | 0.001 |
| **Condition factor (scaled)** | 1 | 0.053 | 1.398 | 0.074 | 1 | 0.024 | 0.894 | 0.195 | 1 | 0.478 | 10.583 | 0.001 |
| **Feed restriction** | 1 | 0.096 | 3.924 | 0.001 | 1 | 0.102 | 6.035 | 0.001 | 1 | 0.284 | 12.050 | 0.001 |
| **Family** | 37 | 1.939 | 9.994 | 0.001 | 37 | 0.721 | 2.200 | 0.011 | 37 | 2.446 | 24.524 | 0.001 |
| **Tank** | 4 | 0.312 | 6.244 | 0.001 | 4 | 0.219 | 7.020 | 0.001 | 3 | 0.276 | 8.643 | 0.001 |
| **Sex** | 1 | 0.035 | -0.118 | 0.548 | 1 | 0.013 | -0.597 | 0.717 | 1 | 0.038 | 1.185 | 0.121 |
| ***vgll3*** | 1 | 0.042 | 0.495 | 0.318 | 1 | 0.018 | 0.108 | 0.461 | 1 | 0.032 | 0.562 | 0.285 |
| ***six6*** | 1 | 0.027 | -0.992 | 0.831 | 1 | 0.013 | -0.617 | 0.739 | 1 | 0.052 | 2.454 | 0.013 |
| **Full model** | 47 | 2.727 | 14.021 | 0.001 | 47 | 1.256 | 7.674 | 0.001 | 46 | 3.929 | 23.997 | 0.001 |
| **Residuals** | 689 | | | | 681 | | | | 724 | | | |

**Table 3**: Variance components for 21 morphological traits obtained from three body planes. $V_A$, $h^2$, and $I_A$ are additive genetic variance, heritability, and evolvability, respectively, after controlling for length, condition factor, feed restriction, and sex.% $V_{A.vgll3}$ and%$V_{A.six6}$ are additive genetic variation explained by the *vgll3* and *six6* loci, respectively (values are truncated to zero if the estimate is less than zero). Values indicate medians, with 95% CI given in parenthesis. % rep. indicate the percent repeatability estimated from repeated measurements of individuals, and to assess the contribution of measurement error to trait measurements.

| Trait [1] | Body Plane[2] | $V_A$ | % $V_{A.vgll3}$ | %$V_{A.six6}$ | $h^2$ | $I_A$[3] | % rep. |
|---|---|---|---|---|---|---|---|
| Dorsal fin | B | 0.0032 (0.0027 - 0.0036) | 2.6 | 0 | 0.083 (0.072 - 0.095) | 0.045 (0.042 - 0.048) | 95.2 |
| Anal fin | B | 7,7e-04 (6.8 e-04, 8.8e-04) | 17.2 | 0 | 0.07 (0.061 - 0.08) | 0.27 (0.26 - 0.3) | 67.3 |
| Pectoral fin | B | 0.0027 (0.0024, 0.003) | 0 | 0 | 0.41 (0.36 - 0.45) | 0.016 (0.015 - 0.017) | 83.7 |
| Tail fin | B | 8.2e-04 (7.3e-04, 9.1e-04) | 0 | 0 | 0.5 (0.47 - 0.54) | 0.051 (0.048 - 0.055) | 69.7 |
| Caudal peduncle | B | 1e-04 (9.1e-05, 1.2e-04) | 0 | 0 | 0.26 (0.24 - 0.29) | 0.02 (0.019 - 0.021) | 65.3 |
| Vertebra thickness | Sml | 1.3e-05 (1.1e-05, 1.5e-05) | 30.7 | 0 | 0.039 (0.033 - 0.045) | 0.31 (0.28 - 0.35) | 63.7 |
| Vertebra thickness | Lrg | 2.0e-05 (1.7e-05, 2.3e-05) | 13 | 0 | 0.06 (0.052 - 0.069) | 0.21 (0.19 - 0.23) | 71.4 |
| Cross section diameter | Sml | 6.8e-04 (5.9e-04, 7.9e-04) | 12.7 | 0 | 0.12 (0.11 - 0.14) | 0.0099 (0.009 - 0.011) | 97.6 |
| Cross section diameter | Lrg | 3.3e-04 (2.9e-04, 3.8 e-04) | 0 | 0 | 0.11 (0.093 - 0.12) | 0.012 (0.01 - 0.013) | 84.1 |
| Aerobic muscle | Sml | 5.8e-05 (5.1e-05, 6.7e-05) | 22.4 | 0 | 0.19 (0.17 - 0.21) | 0.69 (0.62 - 0.76) | 56.5 |
| Aerobic muscle | Lrg | 7.5e-05 (6.6e-05, 8.7e-05) | 0 | 0 | 0.37 (0.34 - 0.41) | 0.72 (0.65 - 0.79) | 24.0 |
| Aerobic muscle vertical extension | Lrg | 0.001 (8.6 e-04, 0.0012) | 22.2 | 2.3 | 0.1 (0.087 - 0.12) | 0.29 (0.26 - 0.32) | 78.5 |
| Eye diameter | B | 3.1e-05 (2.7e-05, 3.5e-05) | 8.6 | 1.6 | 0.11 (0.094 - 0.12) | 0.23 (0.21 - 0.24) | 25.9 |
| Snout length | B | 9.0e-05 (7.9e-05, 1e-04) | 14.1 | 9.4 | 0.12 (0.11 - 0.14) | 0.023 (0.021 - 0.024) | 82.4 |
| Eye vertical position | B | 6.4e-05 (5.6e-05, 7.3e-05) | 0 | 0 | 0.06 (0.052 - 0.069) | 0.15 (0.14 - 0.16) | 79.7 |
| Head length | B | 0.0022 (0.0019, 0.0025) | 0 | 1.8 | 0.22 (0.19 - 0.26) | 0.018 (0.017 - 0.02) | 88.9 |
| Head width | B | 3.5e-05 (3e-05, 4e-05) | 0 | 0 | 0.021 (0.018 - 0.025) | 0.02 (0.019 - 0.022) | 75.4 |
| Body centroid size | B | 0.0034 (0.0031, 0.0038) | 6.3 | 4.2 | 0.47 (0.43 - 0.5) | 7.6e-04 (7,1e-04, 8.2e-04) | 73.8 |
| Head centroid size | B | 5e-04 (4.4e-04, 5.7e-04) | 0.5 | 5.1 | 0.15 (0.12 - 0.17) | 0.009 (0.0084 - 0.0096) | 85.1 |
| Centroid size | Sml | 8.3e-04 (7.2e-04, 9.5e-04) | 4.4 | 0 | 0.27 (0.24 - 0.3) | 0.043 (0.039 - 0.048) | 71.5 |
| Centroid size | Lrg | 0.0014 (0.0012, 0.0016) | 0 | 0 | 0.22 (0.19 - 0.24) | 0.0025 (0.0023 - 0.0028) | 93.5 |

1: Trait length unit is cm for all traits.
2: The trait values are based on landmarks as numbered and indicated in Supplementary Figure 2. B, S, and L prefixes represent body, small cross section, and large cross sections, respectively.
3: $I_A$ is measured as $V_A$ divided by the squared trait mean, and it is unit free.

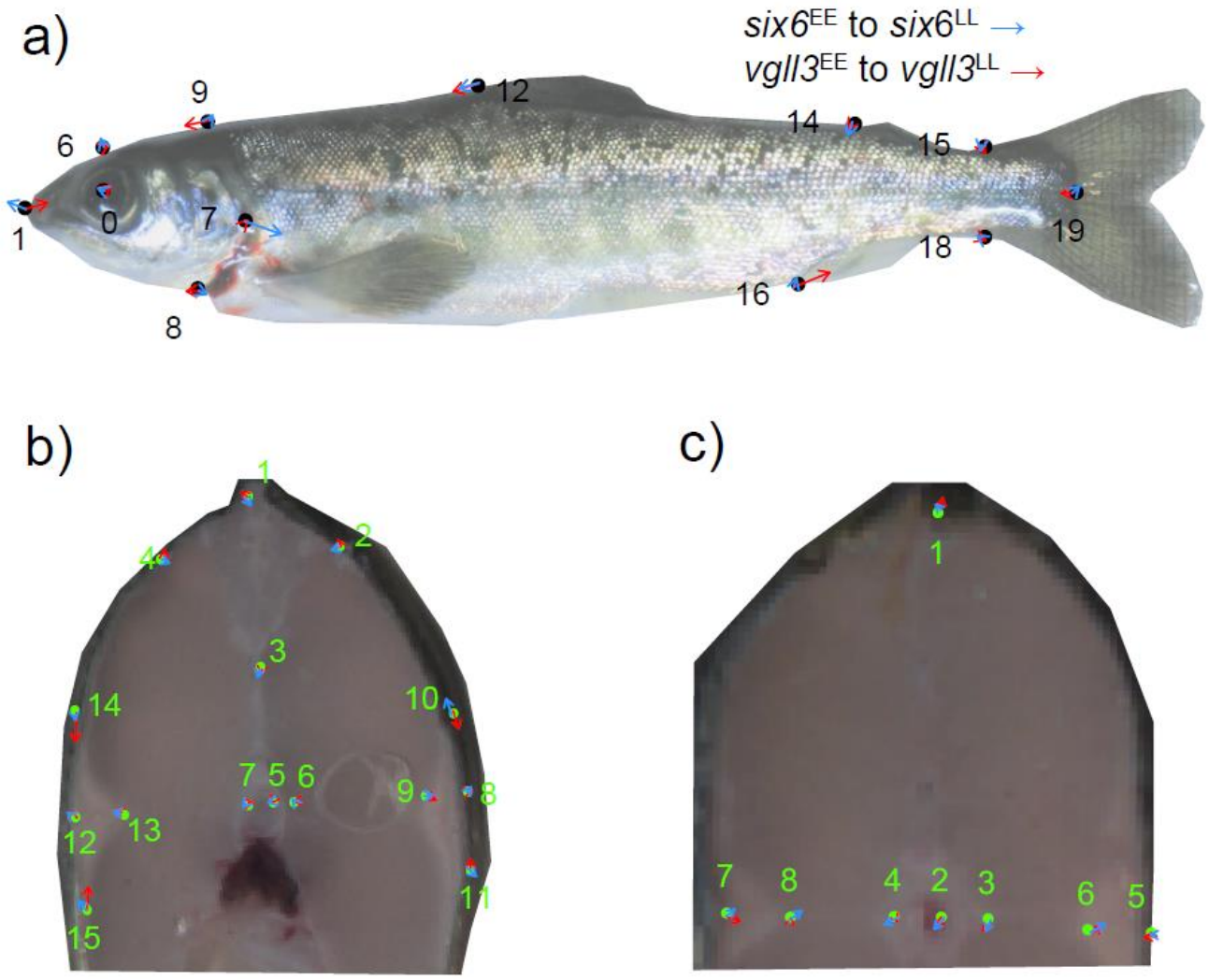


**Figure 1**: The difference between *vgll3*$^{EE}$ and *vgll3*$^{LL}$ (blue lines), and *six6*$^{EE}$ and *six6*$^{LL}$ (red lines) genotypes on body shape of juvenile Atlantic salmon using thin-plate spline in the body (a), and large (b) and small (b) cross sections. The black dots in a, and green dots in b and c are the predicted shape coordinate associated with *vgll3*$^{EE}$ and *six6*$^{EE}$ after the generalized Procrustes analysis. For all images, the effect sizes are magnified by 10x. Landmark numbers are based on Supplementary Figure 2. Note that the body and cross section images are to illustrate the location of landmarks on these body planes, and were slightly distorted to fit onto the average coordinates obtained by Procrustes analysis.

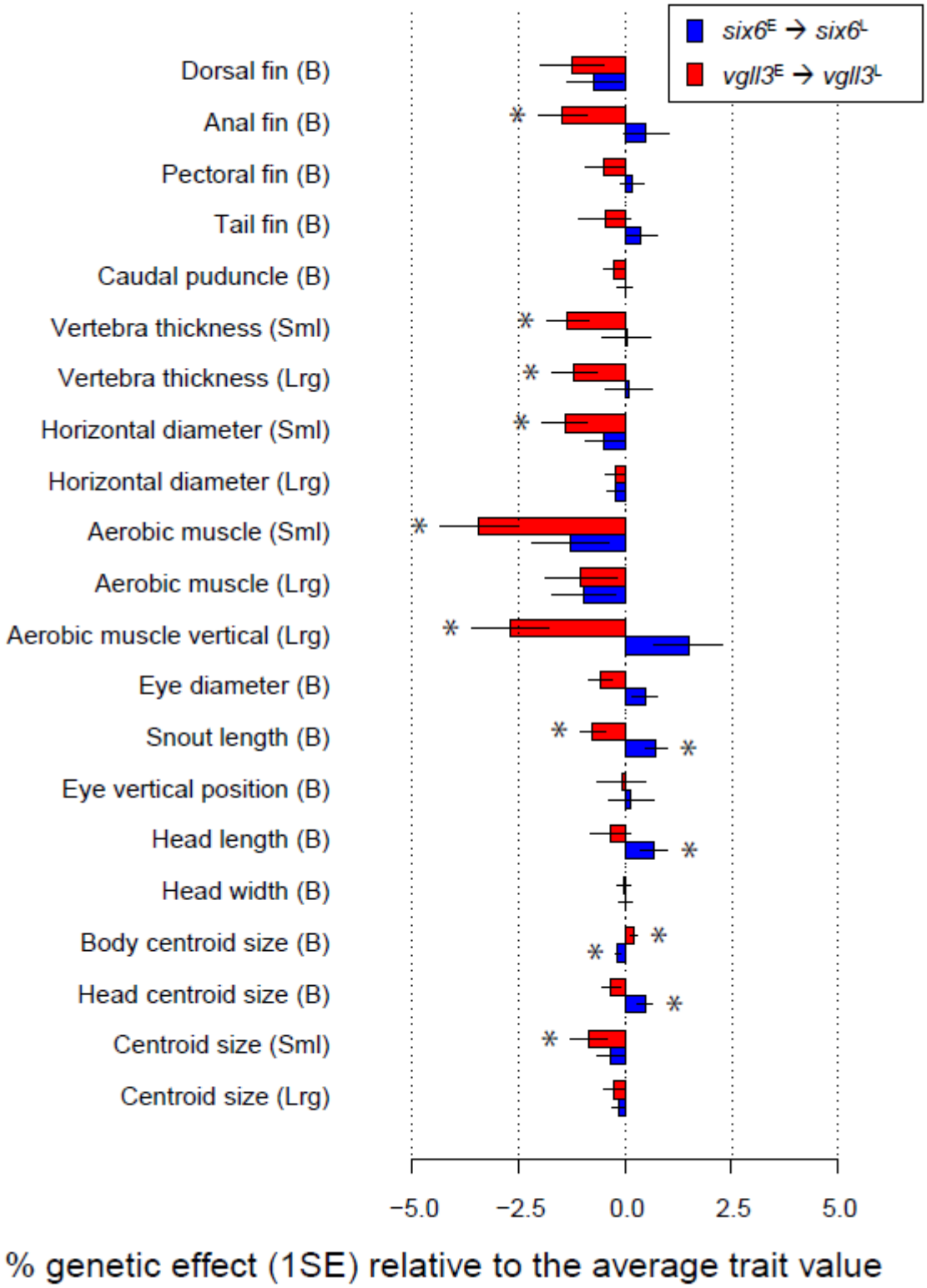


**Figure 2:** Percent trait value change associated with *vgll3*$^{E}$ to *vgll3*$^{L}$ (red lines), and *six6*$^{E}$ to *six6*$^{L}$ (blue lines) allelic substitutions relative to the average trait values. Asterisks denote significant genetic effect. Error bars and 1SE in the x-axis indicate one standard error.